JOURNAL OF Materials CHEMISTRY

Self-assembled gels of liquid crystals: hydrogen-bonded aggregates formed in various liquid crystalline textures

Li Guan and Yue Zhao*

Département de chimie, Université de Sherbrooke, Sherbrooke, Québec, Canada J1K 2R1 and Centre de recherche en science et ingénierie des macromolécules (CERSIM), Université Laval, Québec, Canada G1K 7P4

Received 17th January 2001, Accepted 6th March 2001
First published as an Advance Article on the web 30th March 2001

An azobenzene-containing gelator can gel the nematic liquid crystal BL006 through self-assembly of hydrogen-bonded aggregates. Due to the high nematic–isotropic transition temperature of BL006, the gelation occurs either in the isotropic or the nematic phase depending on the concentration of the gelator. Prior to the aggregation in the nematic phase upon cooling, the gelator can act as a chiral dopant and induce a chiral nematic phase for BL006 over a range of temperatures. This finding has been used to investigate the influence of the liquid crystal environment on the aggregation of the gelator. Making use of rubbed surfaces, electric field and different concentrations of the gelator, various liquid crystalline orientation states, referred to as planar, fingerprint, homeotropic and homogeneous textures, were obtained, and the aggregation of the gelator was allowed to proceed in these environments. It was found that a variety of fibrous and elongated aggregates, differing in morphology and alignment, could be formed, and that the self-assembled liquid crystalline gels with different aggregates could exhibit different electrooptic effects.

Introduction

For a number of low-molecular-weight gelators, a small amount can effectively gel a large volume of organic solvents[1–3] or liquid crystals (LCs),[4–8] resulting in organogels or liquid crystalline gels. Generally, the gelation occurs through the formation of a three-dimensional network self-assembled by fibrous aggregates of the gelator molecules, with the aggregation process driven by specific intermolecular interactions such as hydrogen bonding. Considering the great interest generated by anisotropic gels of liquid crystals stabilized by covalent polymer networks,[9–11] such non-covalent physical gels represent a new type of LC materials and may possess new properties useful for devices applications. For instance, faster response to electric fields was reported for a self-assembled gel of nematic LCs in twisted electrooptic cells;[5] and the possibility of using nematic gels to make flexible twist nematic cells through a continuous process was also proposed.[8] In most cases,[4,5,7] these LC gels have three thermoreversible phases. When a homogeneous mixture is cooled from the isotropic liquid phase, the sol–gel phase transition, determined by the aggregation of the gelator molecules, takes place at a certain temperature and brings the mixture into the liquid gel phase in which randomly dispersed aggregates of the gelator are formed and immobilize the LC compound in its isotropic phase; on further cooling, the liquid gel becomes LC gel as the LC compound enters into its LC phases. However, if the isotropic-to-LC phase transition temperature is relatively high, the gelation can occur in the LC phases. One study found the gelation in the smectic phase[6] and another study showed the gelation in the nematic.[8] One interesting question about the gelation in LC phases is whether the LC environment can affect the aggregation process. In their study using a smectic LC,[6] Kato *et al.* showed that with the LC molecules aligned by rubbed surfaces, the fibrous aggregates formed were located between smectic layers and perpendicular to the rubbing direction. This study demonstrated the influence of the LC orientation on the morphology of the aggregates.

On the other hand, the aggregates formed in the isotropic phase of the LC host may influence the LC alignment in the LC gel state. This was demonstrated by a previous study conducted in this laboratory.[12] A new azobenzene-containing gelator carrying amide groups, AG1, was synthesized and found to be able to gel nematic LCs, such as E7, through H-bonded aggregation of the gelator. Interestingly, for films of E7–AG1 cast on both CaF_2 and glass windows, if the gelation was allowed to occur at temperatures close to the sol–gel phase transition, the aggregation process starts on the edge of the film and the fibrous aggregates grow perpendicularly to the edge. The result of this is that the aggregates are not randomly aligned in the liquid gel state; instead they are well oriented at a macroscopic scale, with the H-bonds aligned in the fibre direction. On cooling into the nematic phase of E7, *i.e.*, into the LC gel phase, the aligned aggregates induce a long-range orientation of the E7 molecules, which is perpendicular to the fibre direction.[12] This self-assembly process thus gives rise to an anisotropic LC gel in the absence of either rubbed surfaces or irradiation that may be applied to affect the azobenzene groups of the gelator molecules. Though the mechanism is still unclear, the study showed how the self-assembled network, if aligned in the liquid gel state, might be used to affect the orientation of the LC molecules in the LC gel phase.

In the case of E7–AG1, as E7 has a quite low nematic–isotropic phase transition temperature $T_{ni} = 58\,^{\circ}C$, the aggregation of AG1 always occurs in the isotropic phase of E7 regardless of the concentration of AG1.[12] If AG1 is used with a nematic LC that has a high T_{ni}, it is possible to see the aggregation of AG1 occurring inside the nematic phase. Having this thought in mind, we have investigated a new system made up from AG1 and BL006. BL006 is a nematic mixture that, similar to E7, is mainly composed of cyanobiphenyl compounds, but has a higher T_{ni} than E7, at about $115\,^{\circ}C$. It was found indeed that the aggregation of AG1 in BL006 could occur in the nematic phase. In addition, what makes this system particularly interesting as compared with the reported systems[5,8] is that prior to the aggregation while being in the nematic phase, AG1 could act as a chiral dopant and induce a chiral nematic phase for BL006. Knowing that a

DOI: 10.1039/b100617g

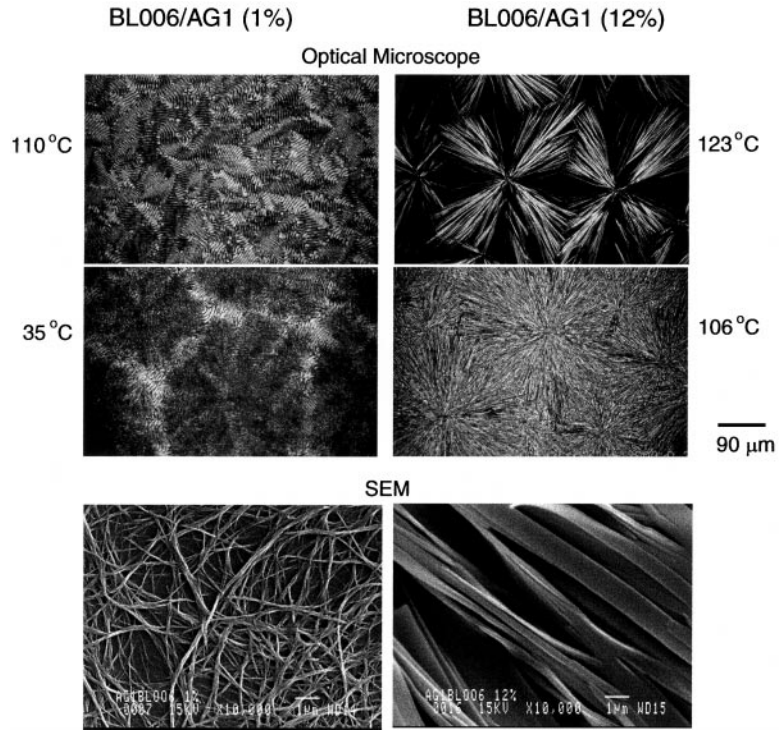

Fig. 1 Polarizing optical micrographs, taken at two temperatures, and SEM pictures (top view), taken at room temperature, for two BL006–AG1 mixtures. For the mixture containing 1% of AG1, the optical micrographs show the gelator-induced chiral nematic phase of BL006 before the aggregation of AG1 in the nematic phase; for the mixture containing 12% of AG1, they show the aggregation of AG1 in the isotropic phase of BL006 before the appearance of the nematic phase. The SEM pictures show the fibrous aggregates of AG1 formed in the chiral nematic phase (with 1% of AG1) and in the isotropic phase of BL006 (with 12% of AG1); the scale bars in the SEM pictures are 1 μm.

variety of liquid crystal textures, *i.e.*, LC orientation states, can be generated for cholesteric (chiral nematic) LCs under the effects of rubbed surfaces and electric field, this system was used to examine the aggregation of AG1 inside different LC environments and to study the influence of the LC orientation on the morphology of the H-bonded aggregates. The results of this study are reported in this paper.

Experimental

The synthesis method for the gelator AG1 has already been reported.[12] Its chemical structure is shown below.

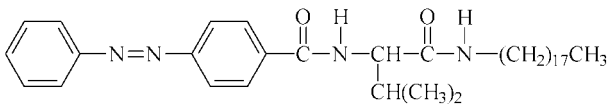

AG1

AG1 has a chiral centre and two amide groups for the formation of intermolecular H-bonds. It is non-mesogenic, and has a melting temperature $T_m = 201\,^{\circ}C$. BL006 was purchased from EM Industries. To prepare a mixture of BL006 and AG1, the calculated amounts of both components were dissolved in THF to make a homogeneous solution; the solvent was then evaporated and the mixture dried in a vacuum oven at 40 °C. Samples used for the microscopic observations were prepared in two ways: 1) thin films (~5 μm) were cast on microscope glass slides whose surfaces were not treated; and 2) mixtures were filled in parallel-rubbed, 4 μm electrooptic cells coated with indium–tin-oxide (ITO) (purchased from Displaytech). In both cases, the mixtures were heated into the liquid phase for the casting or filling process.

The aggregation of AG1 in BL006 was mainly studied by optical microscopy. The micrographs were taken on a Leitz-MP microscope under crossed polarizers; the temperature control was achieved using an Instec hot stage. Typically, each sample was first retained in the liquid phase for more than 5 min for equilibrium, then cooled either at a constant rate into different phases or cooled rapidly to a specific temperature for isothermal annealing. The scanning electron microscopy (SEM) observations were conducted on a JEOL JSC-840A system, and the samples used were prepared by extracting BL006 in hexane. No dissolution of the aggregates was found when the concentration of AG1 was above 0.5 wt%. Differential scanning calorimetry (DSC) and infrared spectroscopy measurements were carried out using a Perkin-Elmer DSC-7 apparatus and a Bomem MB-200 FTIR spectrometer. Finally, the electrooptic effects of the gels were measured at room temperature by means of a photodiode mounted on the polarizing microscope; an ac field (1 kHz) was applied in all cases.

Results and discussion

The sol–gel phase transition temperature is mainly determined by the concentration of the gelator, and mostly insensitive to the medium (solvent or LC) in which the gelator is dissolved.[1–7] It increases with the concentration of the gelator. By contrast, the phase transition temperatures of the LC compound in the gels are little affected by the gelator.[4–7,12] These behaviours were also found for BL006–AG1. As BL006 has a high T_{ni}, the consequence is that for mixtures with relatively low concentrations of AG1, on cooling from the isotropic phase, the aggregation of the gelator molecules occurs only after BL006 undergoes the isotropic–nematic phase transition. Over the temperature range in which BL006 is nematic while AG1 is still isotropic and dissolved in the LC host, the chiral molecules of AG1 induce a chiral nematic phase that is absent for pure BL006. However, if the concentration of AG1 is sufficiently high, the aggregation of AG1 happens before BL006 goes through the isotropic–nematic transition. This property of

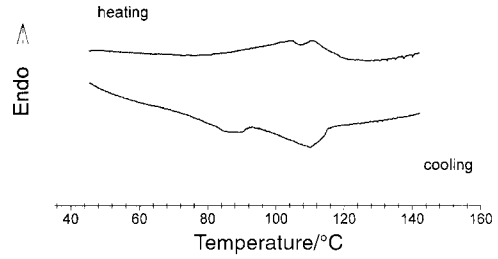

Fig. 2 DSC heating and cooling curves (10 °C min^{-1}) for the BL006–AG1 mixture containing 6% of AG1.

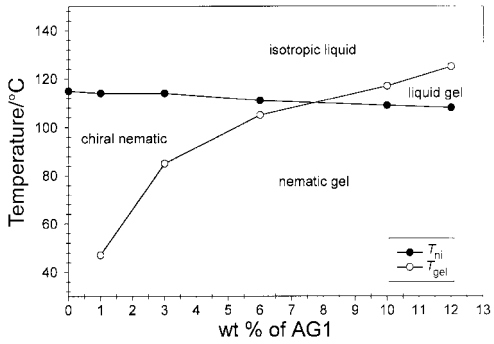

Fig. 3 Phase diagram for BL006–AG1. T_{ni} is the nematic-to-isotropic transition temperature of BL006, and T_{gel} is the gelation (aggregation) temperature of AG1.

BL006–AG1 is illustrated in Fig. 1 which shows some optical micrographs for two mixtures of BL006–AG1 cooled from the isotropic phase, the films being cast on glass slides. For the mixture containing 1 wt% of the gelator, the fingerprint texture of the chiral nematic phase is observed at 110 °C, while at 35 °C the aggregates of AG1 are formed and overlap with the birefringent texture of BL006. The situation is different for the mixture containing 12% of AG1; the fibrous aggregates of AG1, emanating from nucleation centres, are clearly seen at 123 °C while BL006 is still in the isotropic phase and appear dark under crossed polarizers. At 106 °C, BL006 is in the nematic phase, and the birefringent LC molecules fill in the dark areas. The aggregation of AG1 in these two mixtures results in fibrous aggregates of very different morphologies. Fig. 1 also shows the SEM pictures (top view) of the aggregates after extraction of BL006. The aggregates formed in the mixture with 1% of AG1 are thin, rod-like fibres whose diameters are in the range of a couple of hundreds of nanometres, while those formed in the mixture with 12% are flat tapes with widths in the order of 1 μm. The concentration of the gelator appears to be one factor that influences the shape and size of the fibres, but the nature of the phase of BL006, in which the gelation takes place, may be another factor. It was found that thinner and more rod-like fibres were generally obtained through gelation in the chiral nematic phase than in the isotropic phase.

The DSC measurements confirm that for mixtures with low concentrations of AG1, on cooling from the isotropic phase, the nematic phase of BL006 precedes the aggregation of AG1. Fig. 2 shows an example of the results for BL006–AG1 (6%), using a cooling and heating rate of 10 °C min^{-1}. On cooling, the exotherm for the isotropic–nematic transition of BL006 appears first at about 110 °C, followed by the aggregation exotherm of AG1 at about 85 °C. On heating, the melting of the aggregates takes place near 104 °C which is several degrees below the nematic–isotropic transition of BL006 at around 112 °C. As the aggregation of the gelator is mainly a crystallization process, an important supercooling for the sol–gel transition is visible; the location of the aggregation exotherm depends on the cooling rate, moving to higher temperatures for slower cooling rates. Infrared spectroscopy indicates the formation of intermolecular hydrogen bonds in the aggregates of AG1, showing the characteristic bands for two H-bonded C=O groups at 1632 (aliphatic amide) and 1656 cm^{-1} (aromatic amide) once the gelation takes place; before the aggregation, the two bands appear at 1665 and 1681 cm^{-1} for the C=O groups free of H-bonding.

To construct the phase diagram for the system of BL006–AG1, data obtained on a polarizing microscope under a slow cooling rate of 1 °C min^{-1} were utilized; the result is shown in Fig. 3. As the sol–gel transition temperature increases with the concentration of AG1 while the isotropic–nematic transition temperature is little depressed, two different regions can be distinguished. For gelator concentrations below about 7.5%, the three phases are the isotropic liquid, chiral nematic and nematic gel states; for higher concentrations, they are isotropic liquid, liquid gel and nematic gel. In the high-concentration region, after the aggregation of AG1 in the isotropic phase of BL006, on cooling into the nematic phase, no chiral nematic phase was observed. This result suggests that most of the gelator molecules participate in the aggregation in the isotropic phase so that the fraction of the AG1 molecules remaining soluble in the nematic phase is too small to induce a chiral nematic phase. This explanation was supported by an observation for the low-concentration region: on cooling from the chiral nematic phase to the LC gel state, as the aggregation of AG1 progresses, which means more and more AG1 molecules crystallize and no longer act as a chiral dopant for BL006, the fingerprint texture gradually disappears.

What follows describes the use of the gelator-induced chiral nematic phase of BL006 to examine the influence of the LC textures, *i.e.*, the LC orientation states, on the aggregation of AG1. Fig. 4a depicts the three possible LC textures for the mixture containing 6% of AG1 in the parallel-rubbed cell at 110 °C (in the chiral nematic phase). To better illustrate the changes in the LC texture under the effect of an electric field, the viewing area of the cell contains one part coated with ITO and one part without the electrode, being separated by a visible line boundary in the pictures. In the absence of electric field ($E=0$ V), the surface alignment induces a planar texture, for which the axes of the helices formed by the LC directors are normal to the plates (only one helix is drawn in the sketch). Under crossed polarizers, the cell looks bright and uniform; rotating the sample results in no change. When a small voltage of $E=0.7$ V is applied across the cell, the fingerprint texture is formed in the ITO-coated area; for this texture, the helices lie in the plane of the cell, with their axes parallel to the plates. When the applied voltage is raised to $E=1.5$ V, the field is strong enough to unwind the helical structure and align the LC molecules in the field direction, which gives rise to the homeotropic texture appearing dark. Under each of these textures, the mixture could be cooled to lower temperatures to undergo the sol–gel phase transition, and the aggregation of AG1 developed in the specific texture could thus be observed. Fig. 4b shows the fibrous aggregates of AG1 grown in the BL006–AG1 (6%) mixture under the three LC textures. For each texture, the pictures were taken at two temperatures, first at 104 °C, which was close to the sol–gel transition temperature, after the sample was retained at this temperature for about 30 min; and then at room temperature (25 °C) after the sample was slowly cooled. At room temperature, the much more birefringent appearance of BL006 makes it difficult to compare the fibres. Therefore, in order to view the aggregates of AG1, a voltage was applied in all cases to reorient the LC molecules in the field direction so that a black background was obtained. From the pictures, the H-bonded aggregates formed in the various LC environments do not look dramatically different, but do differ in some aspects. Under the planar texture, the fibres seem to be thicker and straighter than those

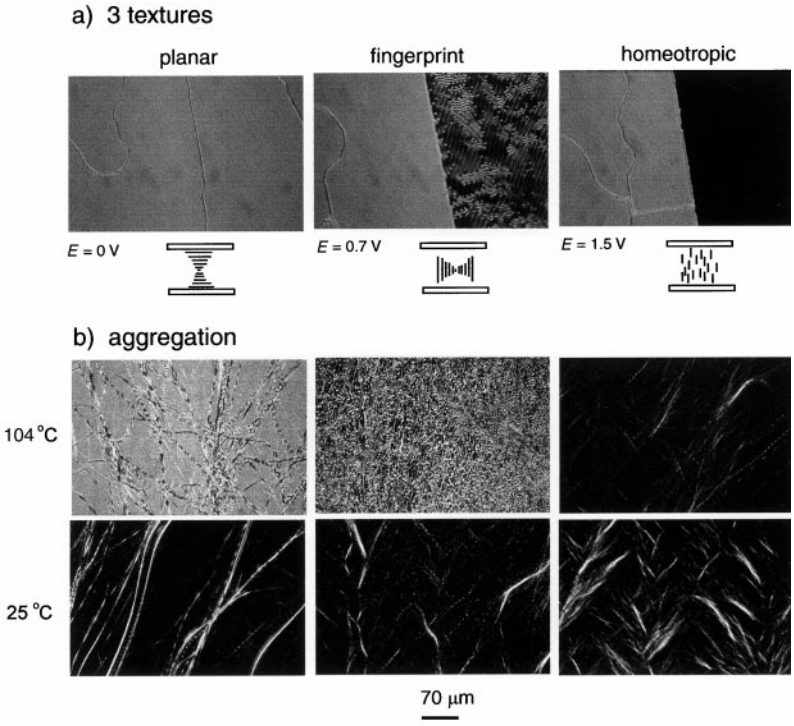

Fig. 4 Polarizing optical micrographs for the mixture of BL006–AG1 (6%) in a 4 μm, parallel-rubbed electrooptic cell, showing a) the three liquid crystalline textures that can be obtained, before aggregation, with or without a voltage applied across the cell; and b) the fibrous aggregates of AG1 formed under three liquid crystalline textures. For the pictures at 25 °C, the dark background was obtained by applying a voltage across the cell to align the BL006 molecules.

formed in the fingerprint and homeotropic textures. By contrast, the aggregates in the homeotropic texture are feathered thin fibres.

An interesting feature that can be noticed in all cases is that some fibres appear broken along the fibre direction. This is particularly visible on the bright background of the planar texture at 104 °C, with some fibres looking like "a string of pearls". This appearance is not characteristic for fibres formed in a chiral LC environment since it can also be seen for the homeotropic texture. Rotation of crossed polarizers results in no change in the positions where the fibres appear dark. Those observations suggest that these apparently discontinuous fibres may reflect the mechanism of the fibre growth. Fig. 5 shows a SEM picture for fibres formed under the planar texture (the cell was carefully opened after the extraction of the LC). A three-dimensional network formed by the fibrous aggregates (100–200 nm in diameter) is visible. In addition, it can be noticed that many fibres do not have a uniform thickness, which is more prominent for thinner fibres such as the one marked by an arrow deeper in the background of the figure. One possible mechanism is that the fibre growth proceeds by coalescence of the aggregate particles, which forms "necks" between touching

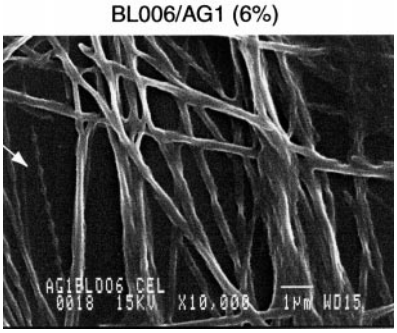

Fig. 5 SEM picture (top view) for the aggregates of AG1 formed in the mixture of BL006–AG1 (6%) under the planar texture; a thin fibre is marked by a white arrow. A 1 μm scale bar is shown on the picture.

droplets. Since some of the thin "necks" may appear invisible on an optical microscope, the fibres appear discontinuous. As the aggregation process develops in time, the condensation of thin fibres may result in large fibres having more uniform thickness. Finally, two observations should be mentioned for the mixture containing 6% of AG1. First, if the mixture is cooled quickly from the liquid phase to room temperature, the fast nucleation and growth leads to spherical, star-like aggregates, similar to those for the mixture with 12% of AG1 (Fig. 1), regardless of the LC texture under which the aggregation occurs. Secondly, it was found that on cooling from the liquid phase, the aggregation temperature was not affected by the LC texture.

The helical pitch of an induced chiral nematic phase generally increases as the concentration of the chiral dopant decreases.[13] This is also the case for BL006–AG1. When the concentration of AG1 is lowered to below about 3.5%, the half-pitch length is larger than the 4 μm gap of the electrooptic cell and, consequently, no planar texture can be obtained. Instead, the LC molecules are uniaxially aligned by rubbed surfaces in the plane of the plates, leading to the homogeneous LC texture. The mixture of BL006–AG1 (3%) was used to observe the aggregation process under both the homogeneous and homeotropic textures. Similar to BL006–AG1 (6%), a voltage was applied across the cell to make the homeotropic LC orientation. Presented in Fig. 6 are optical micrographs that show the aggregates observed under these conditions. On the one hand, pictures from a) through c) illustrate the growth of an aggregate under the homogeneous texture. The cell was isothermally annealed at 80 °C with the first picture taken after 5 min at this temperature and the subsequent pictures recorded with a 1 minute interval. The aggregate is not fibrous; rather it has a rectangular shape. Emerging from a spherical central point at the beginning, it grows with two main trunks that are crossed and make an angle of about 60° to the LC orientation (surface rubbing) direction. The dendritic growth proceeds mainly at a right angle to the rubbing direction; in other words, the growth is hindered in the LC orientation

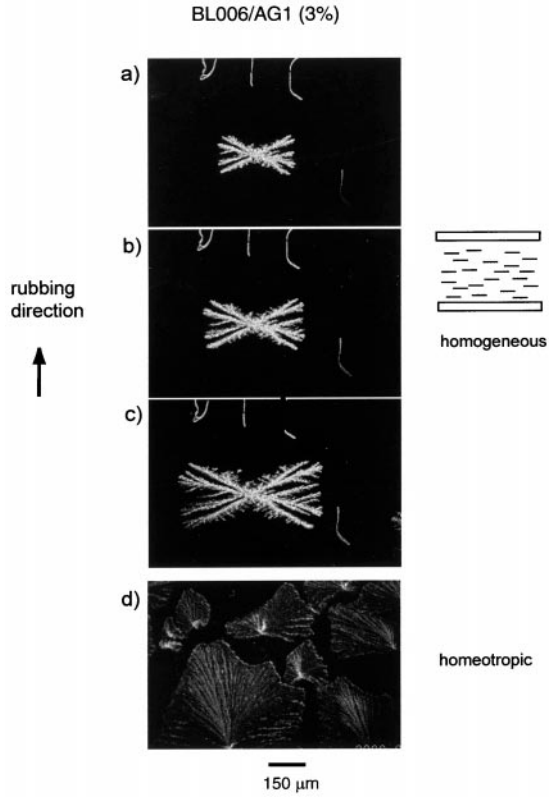

Fig. 6 Polarizing optical micrographs showing the growth of an elongated aggregate of AG1 in the mixture of BL006–AG1 (3%) under the homogeneous liquid crystal orientation state (pictures a–c) as well as the aggregates formed under the homeotropic orientation. The surface rubbing direction is indicated.

direction. Interestingly, the size of the aggregate increases in time, but the rectangular shape remains unchanged with a constant axial ratio of 2. At lower aggregation temperatures, similar results were obtained, but the axial ratio decreases. Picture d) in Fig. 6 is the top view of the aggregates formed under the homeotropic LC orientation. In this case, since the LC molecules were aligned normal to the picture, the slowdown of the growth in the LC orientation direction cannot be seen. The aggregates formed in the plane of the cell have irregular shapes. Unlike the mixture containing 6% of AG1, under both textures no fibrous aggregates could be obtained for the mixture containing 3% of AG1.

When the concentration of the gelator is further lowered in the mixture, an even greater variety of aggregates can be obtained. The shape and size and number of the H-bonded aggregates were found to be particularly sensitive to the aggregation temperature for the mixture containing 1% of AG1. Fig. 7 shows a set of optical micrographs for aggregates developed under both the homogeneous and homeotropic textures at three temperatures. Under the homogeneous LC orientation, at 45 °C, fewer aggregates were formed, but, similar to the mixture containing 3% of AG1, they have an elongated shape with their long axes aligned perpendicularly to the LC orientation. Again, two main trunks emanating from the centres can be noticed, only this time they are orthogonal. At 40 °C, which was just 5 °C lower, more but smaller aggregates were obtained. They are still highly elongated, but, contrary to the aggregates formed at 45 °C, they align their long axes along the LC orientation direction. At 25 °C, a large number of small aggregates were obtained. However, they no longer have elongated shapes, and are randomly dispersed in BL006. Under the homeotropic LC orientation, since the top view sees the aggregates in the plane perpendicular to the LC orientation direction, it can be expected that any faster or

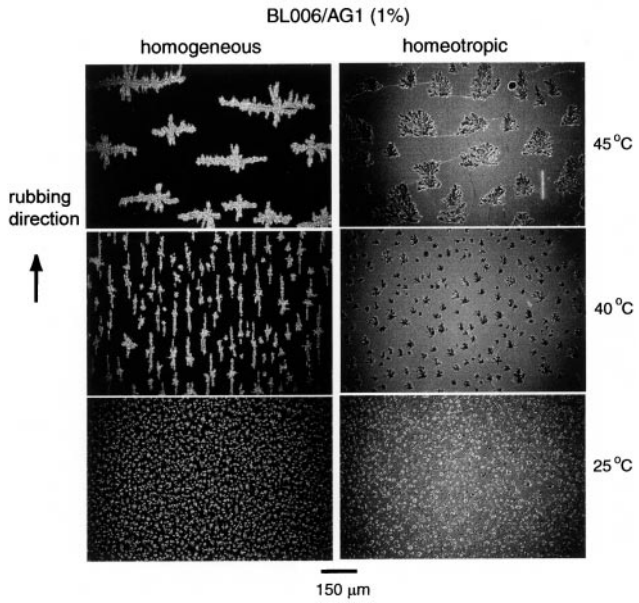

Fig. 7 Polarizing optical micrographs showing the aggregates of AG1 of various morphologies and alignments in the mixture of BL006–AG1 (1%) at three temperatures and under both the homogeneous and homeotropic textures. The surface rubbing direction is indicated.

slower rate of aggregation in this direction cannot be revealed. This is indeed the case as can be noticed from Fig. 7. The observed cross sections of the aggregates have irregular shapes. For each temperature, the number and size of the aggregates formed under the homeotropic texture corroborate the results for the aggregates formed under the homogeneous orientation.

The whole of the above results indicates that the formation of the H-bonded aggregates of AG1 in the LC host BL006 is influenced by a number of factors that include the concentration of the gelator, temperature and the LC orientation state. With 6% of AG1, long fibrous aggregates form a network structure in the planar, fingerprint and homeotropic textures. By contrast, lower concentrations of AG1 give rise to stand-alone aggregates of elongated shapes developed in oriented LC environments. With 3% of AG1, the aggregates align their long axes perpendicular to the LC orientation, while with 1% of AG1 they can be aligned either parallel or perpendicular depending on the aggregation temperature. At this point, we have no explanation for these interesting but puzzling observations. More studies are needed to understand the process of aggregation under the different conditions. Nevertheless, the results show that the oriented LC environment can be used to affect the shape and alignment of the H-bonded aggregates.

The electrooptic effects for the gels with aggregates of AG1 formed in various LC textures or orientation states were investigated at room temperature under crossed polarizers. For all the measurements, the cell was placed with the rubbing direction at 45° to the polarizers. The transmittance of light is generally lower for the gels than pure BL006. This is caused by the interaction between the LC and the aggregates, which diminishes the degree of the LC orientation induced by rubbed surfaces. Fig. 8 shows the plots of the transmittance of light as a function of applied voltage for the gels containing 6% of AG1, whose preparations were described in Fig. 4, as well as for pure BL006. All the gels respond to the field at similar voltages as compared to pure BL006, but the decrease in the transmittance is more gradual. On the other hand, the contrast is lowered by the presence of the aggregates, with the highest effect for the sample prepared under the fingerprint texture and similar effects for the samples obtained under the planar and homeotropic LC orientation states. In all cases, when the

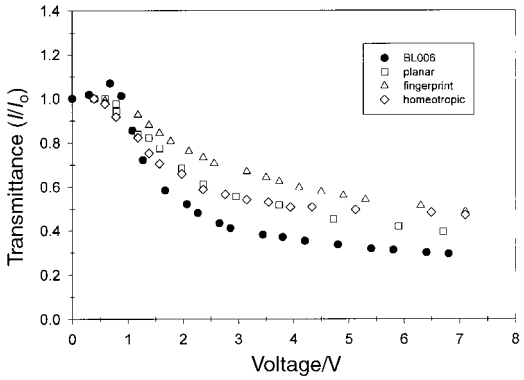

Fig. 8 Transmittance of light *versus* applied voltage for pure BL006 as well as the gels prepared from the mixture of BL006–AG1 (6%) having the aggregates of AG1 developed under the planar, fingerprint and homeotropic textures.

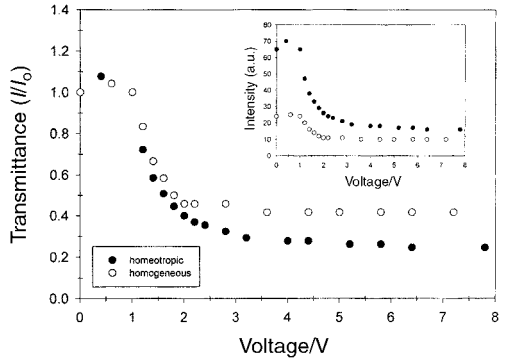

Fig. 9 Transmittance of light *versus* applied voltage for two gels prepared from the mixture of BL006–AG1 (1%) having the aggregates of AG1 formed at 40 °C and under the homogeneous and homeotropic textures. The inset shows the relative transmitted light intensities for the two gels.

voltage is decreased, the change in transmittance is reversible with little hysteresis (data not shown for the sake of clarity).

For mixtures with lower concentrations of AG1, the electrooptic effects are more dependent on the morphologies of the aggregates formed under the homogeneous and homeotropic textures. An example of the results is given in Fig. 9 which compares the gels with 1% of AG1 prepared under both LC orientation states at 40 °C (Fig. 7). In addition to the plots of the transmittance *versus* voltage, the inset shows the relative transmitted light intensities for the two gels. For the gel prepared under the homogeneous orientation, the elongated aggregates formed in the plane of the cell diminish the degree of the LC orientation in the rubbing direction. The LC molecules entrapped by the aggregates and unable to align under the surface effect cause the bright appearance of the aggregates, which explains the low transmission of light before the application of the voltage. For the gel obtained under the homeotropic orientation, the aggregates, aligning their long axes along the LC orientation direction, are mainly isotropic in the plane of the cell and have small sizes; they may have less interaction with the LC molecules so that the latter can well be aligned by rubbed surfaces once the electric field is turned off. This leads to a higher transmission of light. The gel prepared under the homeotropic orientation has not only a much higher light transmission but also a larger contrast than the gel prepared under the homogeneous orientation. Moreover, in contrast to the gels containing 6% of AG1, the samples with 1% of aggregates show a sharp decrease in transmittance as the voltage is applied, with a threshold voltage that seems even slightly lower than that of pure BL006.

Conclusions

The aggregation of AG1 in the high-T_{ni} nematic liquid crystal BL006 can occur in the nematic phase. Prior to the aggregation, the gelator acts as a chiral dopant and induces a chiral nematic phase. Making use of rubbed surfaces, electric field and changes in the concentration of AG1 in the mixtures, it is possible to observe the aggregation of AG1 under various liquid crystalline orientation states, referred to as planar, fingerprint, homeotropic and homogeneous textures. These liquid crystalline textures can influence the hydrogen-bonded aggregates of AG1. Combined with the effects of the aggregation temperature, a variety of morphologies were obtained, including fibrous and elongated aggregates with different alignments. The electrooptic effects of these gels may be affected by the aggregates of AG1.

Acknowledgements

We would like to thank M Pierre Magny for assisting the electron microscopy observations. Financial support from the Natural Sciences and Engineering Research Council of Canada and the Fonds pour la Formation de Chercheurs et l'Aide à la Recherche of Québec is acknowledged.

References

1 P. Terech and R. G. Weiss, *Chem Rev.*, 1997, **97**, 3133.
2 C. Geiger, M. Stanescu, L. Chen and D. G. Whitten, *Langmuir*, 1999, **15**, 2241.
3 K. Hanabusa, R. Tanaka, M. Suzuki, M. Kimura and H. Shirai, *Adv. Mater.*, 1997, **9**, 1095.
4 T. Kato, G. Kondo and K. Hanabusa, *Chem. Lett.*, 1998, 193.
5 N. Mizoshita, K. Hanabusa and T. Kato, *Adv. Mater.*, 1999, **5**, 392.
6 N. Mizoshita, T. Kutsuna, K. Hanabusa and T. Kato, *Chem. Commun.*, 1999, 701.
7 K. Yabuuchi, A. E. Rowan, R. J. M. Nolte and T. Kato, *Chem. Mater.*, 2000, **12**, 440.
8 R. H. C. Janssen, V. Stumpflen, C. W. M. Bastiaansen, D. J. Broer, T. A. Tervoort and P. Smith, *Jpn. J. Appl. Phys.*, 2000, **39**, 2721.
9 D. K. Yang, L. C. Chien and Y. K. Fung, in *Liquid Crystals in Complex Geometries Formed by Polymer and Porous Networks*, ed. G. P. Crawford and S. Zumer, Taylor & Francis, London, 1996, p. 103.
10 R. A. M. Hikmet, *J. Mater. Chem.*, 1999, **9**, 1921.
11 Y. Zhao and Y. Chenard, *Macromolecules*, 2000, **33**, 5891.
12 L. Guan and Y. Zhao, *Chem. Mater.*, 2000, **12**, 3667.
13 S. Kurihara, S. Nomiyama and T. Nonaka, *Chem. Mater*, 2000, **12**, 9.